Dynamic phase converter for passive control of combustion instabilities

N. Noiray, D. Durox, T. Schuller and S. Candel

EM2C Laboratory, CNRS and Ecole Centrale Paris,
92295 Châtenay-Malabry, FRANCE

Abstract

This article proposes a novel strategy for controlling acoustic-combustion instabilities. It is specifically designed for systems comprising a collection of flames like those found in radiant burners, silo combustors and some gas turbine chambers. The onset of oscillations is suppressed over a broad range of frequencies by modifying the dynamics of the flame collection to obtain a neutral response to incident perturbations. This is achieved in one practical implementation by inserting a Dynamic Phase Convertor (DPC) in a burner comprising a large number of injection channels. The DPC system imposes an out of phase motion of perturbed individual flames, yielding opposite heat release fluctuations which compensate each other and yield a steady response to incoming perturbations. The DPC principle is demonstrated both numerically and experimentally in a configuration comprising a collection of small laminar premixed flames. Simulations show that the flame dynamics is that expected theoretically and that the practical implementation operates as planned even under slightly off-design conditions. It is concluded that the concept could have a wide range of application. Practical implementations are the subject of a patent pending.

Keywords: combustion instabilities, passive control, multipoint injection, flame dynamics

1. Introduction

Combustion instabilities constitute a serious problem in a wide range of industrial applications because they enhance noise levels, induce structural vibrations, intensify heat fluxes to the boundaries and in extreme cases lead to damage and even destruction of the system. Unstable combustion due to a resonant coupling between unsteady heat release and system acoustics have been extensively investigated and a substantial effort has been expanded to actively [1, 2] or passively [3, 4] control the resulting oscillations. Compared to active control solutions, passive methods have the advantage of being more reliable and independent of an external source of energy and thus raising less problems. They are also easier to implement and therefore widely used in practice.
Passive methods modify the balance of acoustic energy by reducing the gain or increasing losses

This is a pre-print version. Published in *Proceedings of the Combustion Institute*, Volume 32 (2009), p. 3163-3170, DOI: 10.1016/j.proci.2008.05.051

to hinder perturbation growth. One can generally distinguish two classes of methods. In the first group, acoustic energy dissipation is augmented by liners, bias flow perforated screens [5, 6], Helmholtz or quarter wave resonators [7, 8, 9].
The second group of methods is aimed at reducing the efficiency of driving processes. This is achieved by changing the injector geometry and the flame dynamics. This principle is applied for example to suppress large scale coherent vortices which are periodically shed under unstable operation, roll-up the flame and lead to large excursions in heat release rate, a process illustrated in [10]. The amplitude level of these vortex structures may be reduced for example, by employing multistep geometries [3] which generate smaller scale structures that do not sustain flow oscillations. Similarly small scale vortex generators are proposed to brake the larger structures and avoid resonant coupling [11, 12]. It is also argued that injectors with noncircular cross section could be used to enhance mixing by accelerating the decay of annular vortices [13]. In reference [14], two burners are staggered with respect to each-other in a ramjet configuration to modify the convective wavefront patterns in the flame merging region and thus to reduce the amplitude of the coherent response of the global reaction zone. Another method consists in adjusting injection positions inside the manifold feeding of an arrangement of multiple flames in order to counteract coupling involving equivalence ratio fluctuations [15, 16].
The novel method presented in this article belongs to the second class of strategies. It consists in modifying the flame dynamics to obtain a neutral response to perturbations. In distinction with acoustic dampers which enhance dissipation, the method relies on a "Dynamic Phase Converter" (DPC) acting on the underlying causes. The DPC principle explained in section 2 is demonstrated by numerical simulations and verified subsequently by external modulation experiments (section 3) and by control of autonomous oscillations (section 4). The concept, illustrated in a laminar configuration with a geometry close to that found in radiant burners, is more general and could be extended to other applications involving larger scale turbulent flames.

2. DPC principle

Industrial combustors often feature multiple flames in an arrangement which can be modified to obtain a neutral response to incoming perturbations. This is achieved by the DPC which imposes a phase lag between one half of the flames and the other half. This induces out of phase flame motions and mutual compensation resulting in a neutral response of the global reaction zone in terms of heat release rate.
The DPC principle is materialized in Fig. 1 by one possible geometrical arrangement. One distinguishes in this drawing injectors of type 1 and 2 providing the out of phase response to incident acoustic perturbations. It is known that the flames are sources of acoustic energy when they respond to flow velocity perturbations. The central idea of the DPC is to modify within a short distance (of the order of the injection system size) the phase angle of such incident perturbations, which modulate the low Mach number flow inside the feeding channels of diameter d_p, to induce a

This is a pre-print version. Published in *Proceedings of the Combustion Institute*, Volume 32 (2009), p. 3163-3170, DOI: 10.1016/j.proci.2008.05.051

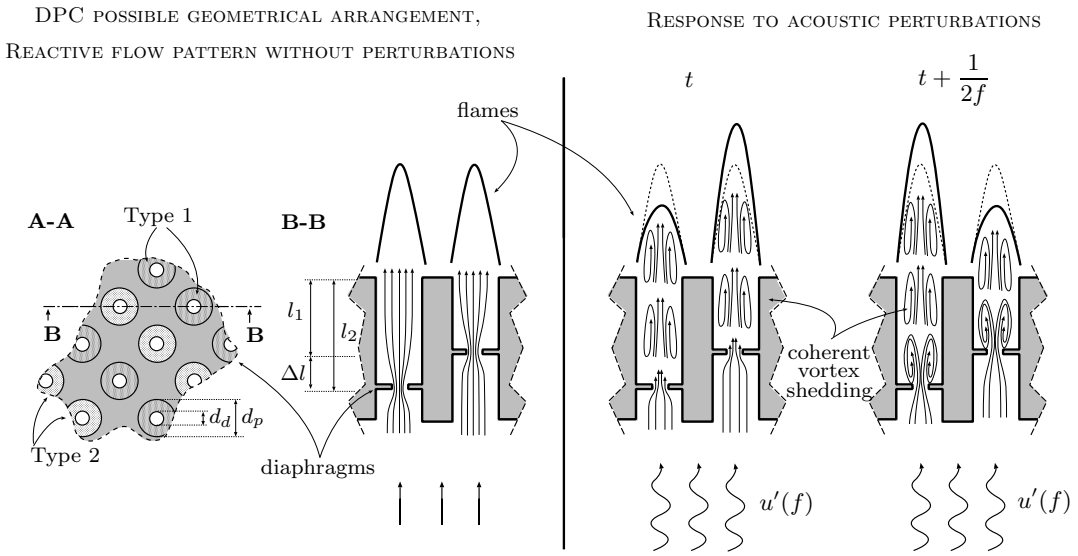

Figure 1: Schematic representation of the dynamic phase convertor (DPC) system proposed to control combustion oscillations. Diaphragms are included in the channels composing the multipoint injection. The diaphragms are staggered in the axial direction. This is used to introduce a phase shift in the perturbations convecting in the channels. The stagger Δl is suitably adjusted as explained in the text.

phase delayed response of the flames. Since acoustic wavelengths of interest ($\lambda_{ac} = c/f$) are quite long it is not possible to obtain a sizeable phase shift with an acoustic delay line. One may however circumvent this problem by first converting the incoming perturbation into a convective mode. This is achieved by means of diaphragms inside the feeding channels of diameter d_p constricting the flows to a diameter d_d as illustrated in Fig. 1. When acoustic modulations impinge on the diaphragms from upstream coherent vortices are shed in the confined jets shear layers established from the diaphragm apertures. The convection velocity $\mathcal{U}_{cv}$ of these hydrodynamic perturbations is typically close to the mean flow velocity $\bar{u}_d$ in the orifice. One can write $\mathcal{U}_{cv} = \alpha\bar{u}_d = \alpha\beta(d_p/d_d)^2\bar{u}_0$ where $\bar{u}_0$ is the mean flow velocity at the channels inlet. Experiments carried out on a scaled up system indicate that $k = \alpha\beta \simeq 0.95$ for a wide range of Strouhal numbers $0.3 < fd_p/\bar{u}_0 < 1$. Considering that the Mach number inside the feeding channels is small $M \ll 1$, the vortex train wavelength $\lambda_{cv} = \mathcal{U}_{cv}/f$ is much shorter than the acoustic wavelength λ_{ac}, and it is then easier to obtain significant phase delays between the incident acoustic perturbation and the resulting hydrodynamic disturbance within a short distance. It is then clear that the convective mode can be used effectively to obtain a differential phase between the different injection channels.
This is accomplished by using staggered positions for the diaphragms in the type 1 and 2 injectors

This is a pre-print version. Published in *Proceedings of the Combustion Institute*, Volume 32 (2009), p. 3163-3170, DOI: 10.1016/j.proci.2008.05.051

(see Fig. 1). The phase lag $\Delta\varphi$ obtained in this way is given by :

$$\Delta\varphi = 2\pi f \frac{\Delta l}{\mathcal{U}_{cv}} = 2\pi f \frac{\Delta l}{k(d_p/d_d)^2 \bar{u}_0} \tag{1}$$

where Δl is the stagger distance. If the system is expected to oscillate around an eigenfrequency f_n, the stagger distance must be chosen to yield an optimum dynamic compensation of heat release fluctuations, i.e. $\Delta\varphi = \pi$:

$$\Delta l = \frac{k(d_p/d_d)^2 \bar{u}_0}{2f_n} \simeq \frac{(d_p/d_d)^2 \bar{u}_0}{2f_n} \tag{2}$$

where f_n designates the nominal resonant frequency. With this design, one flame is stretching while the next flame is retracting (right side of Fig. 1). The coherent motion of the flame fronts is precluded and a vanishing amount of acoustic energy is fed in the oscillation hindering its growth. The global heat release rate remains quasi-steady even if individual heat release rates of each flame fluctuate in response to incident acoustic perturbations. In a natural regime of operation and in the absence of upstream perturbations, the system is in a steady state and the flow simply adapts to the presence of diaphragms. This situation is depicted on the left side of Fig. 1. Positions l_1 and l_2 are defined (Fig. 1) in part as a function of the diameter ratio d_d/d_p and of the mean flow rate per channel in order to reattach the jets to the side walls inside the type 1 and 2 channels. The geometry guarantees that head losses in the two types of channels are nearly equal. In the steady state the flames established on the two types of channels are nearly identical as illustrated in Fig. 1.

Numerical simulations, initially carried out to validate the previous concept are briefly described in the next section. The promising results obtained numerically served to develop a prototype, which was then tested in a configuration featuring well-documented unstable regimes [17, 18]. To show that the DPC effectively operates over a broad band around the nominal frequency f_n the choice was made to present results under slightly different geometrical and flow conditions. Stabilization achieved by the DPC is optimum for $\Delta\varphi = \pi$, but its effects are also retrieved for neighboring values of the phase lag. It is also worth noting that a possible drawback of this system is that it may effectively suppress the thermo-acoustic coupling over a broad range around the nominal frequency f_n but that another mode may appear outside this range and define the dynamics of the system. This issue is commonly encountered in other types of passive control devices. In the present case, it will be shown in section 4 that higher frequency eigenmodes arise ($f > 2$ kHz), but these modes feature a substantially lower amplitude and could be suppressed by placing additional dampers like bias flow perforated plates or acoustic liners.

3. System response to acoustic perturbations

The DPC concept is here investigated under external modulation. This section begins with numerical simulations and then reports results of experiments.

This is a pre-print version. Published in *Proceedings of the Combustion Institute*, Volume 32 (2009), p. 3163-3170, DOI: 10.1016/j.proci.2008.05.051

3.1. Numerical simulations

Calculations are carried out with the AVBP code now commonly used to simulate compressible reactive flows mainly for Large Eddy Simulations of turbulent combustion (e.g. [19, 20]). AVBP is also adapted to simulations of laminar flames dynamics at low Reynolds numbers. It is less precise than higher order DNS solvers, but can be used to investigate complex geometries with unstructured meshes, which is specifically interesting here.
The three dimensional mesh considered in this study (Fig. 2) includes 4 655 000 tetrahedral cells. The geometry includes (1) An upstream volume fed by a lean methane-air mixture ($\phi = 0.86$) at ambient temperature (300 K) (2) Two injection channels ($d_p = 2$ mm) equipped with diaphragms (orifice diameter $d_d = 1.2$ mm) located at staggered positions and (3) A downstream volume in which combustion takes place. Each channel anchors a conical flame. The array of channels and conical flames considered experimentally is thus described by considering two channels side by side and employing periodicity conditions on the lateral sides of the inlet and outflow volumes (see Fig. 2).

The unsteady flow is laminar and the Navier-Stokes equations are integrated without spatial filtering and subgrid scale models. Mesh refinement is enforced in particular regions to provide an accurate description of the injection channels boundary layers, the annular vortices coherently shed from the diaphragm lips and the flames fronts.
To retrieve the flame dynamics it is not necessary to use a detailed kinetic scheme. For the lean mixture considered, a single step reaction suffices to yield accurate values for the laminar burning velocity, flame thickness and hot products temperature. The volumetric rate of reaction $\dot{\omega}$, given in $\mathrm{mol\,m^{-3}\,s^{-1}}$ is defined by an Arrhenius law :

$$\dot{\omega} = A\Big(\frac{\rho Y_{CH_4}}{W_{CH_4}}\Big)^{\nu_{CH_4}}\Big(\frac{\rho Y_{O_2}}{W_{O_2}}\Big)^{\nu_{O_2}} \mathrm{e}^{-E_a/RT} \tag{3}$$

The pre-exponential factor, activation energy and exponants $A = 1.1\,10^{10}$ S.I., $E_a = 20\,\mathrm{kJ\,mol^{-1}}$, $\nu_{CH_4} = 1$ and $\nu_{O_2} = 0.5$ yield a laminar burning velocity $S_L = 0.303\,\mathrm{m\,s^{-1}}$ which is close to measurements ($S_L = 0.317\,\mathrm{m\,s^{-1}}$ for $\phi = 0.86$) carried out in ref. [21].
A flat velocity profile $\bar{u}_i = 0.65\,\mathrm{m\,s^{-1}}$ is imposed to the inlet section. A harmonic modulation u_i' at $f = 650$ Hz is added to the mean velocity with an amplitude fixed to $0.15\,\bar{u}_i$. The outlet section allows outward propagation of acoustic waves without reflection. This is achieved by using non-reflecting NSCBC conditions [22]. No-slip isothermal wall conditions ($T = 600$ K) are imposed to the injection system.
A Lax-Wendroff second order scheme is first used to initiate combustion (without modulation) and next to reach an oscillatory steady state. Calculations are then pursued with a Taylor-Galerkin Compact scheme providing third order accuracy and designated as TTGC [23] over four established periods of oscillation.

The mean velocity at the channel inlet $\bar{u}_0$ is equal to $1.9\,\mathrm{m\,s^{-1}}$ and the corresponding Reynolds

This is a pre-print version. Published in *Proceedings of the Combustion Institute*, Volume 32 (2009), p. 3163-3170, DOI: 10.1016/j.proci.2008.05.051

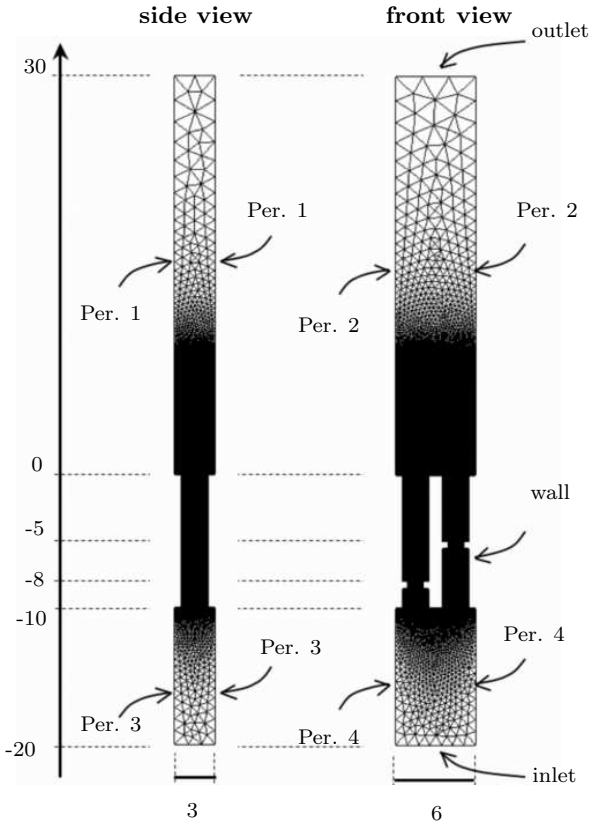

Figure 2: Boundary conditions and mesh geometry and footprint (dimensions in mm). Channels and diaphragms diameters are respectively equal to 2 and 1.2 mm.

This is a pre-print version. Published in *Proceedings of the Combustion Institute*, Volume 32 (2009), p. 3163-3170, DOI: 10.1016/j.proci.2008.05.051

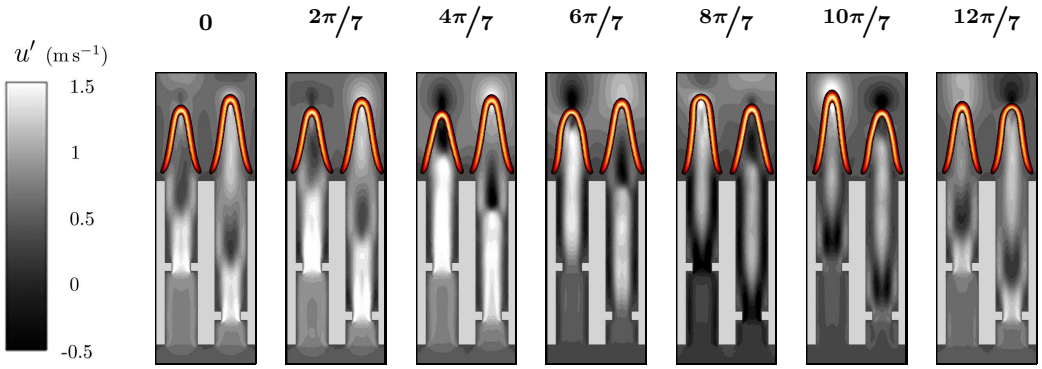

Figure 3: Numerical simulation of the phase-converter response to a global acoustic excitation (f = 650 Hz). Extracted slices of the 3 dimensional computation. The volumetric reaction rate is shown on a colour scale. The distribution of **axial** velocity fluctuation u' is displayed on a scale of gray levels. The sequence corresponds to 7 successive phases during a cycle of oscillation.

and Strouhal numbers are $Re = \bar{u}_0 d_p/\nu = 253$ and $St = f d_p/\bar{u}_0 = 0.68$. This also gives a Strouhal number based on the diaphragm diameter $St_d = f d_d/\bar{u}_d = 0.14$. It is known [24] that at such values of the Strouhal number the jet is quite susceptible to acoustic perturbations and that incident acoustic fluctuations are efficiently converted into a convective mode. Results presented in Fig. 3 show the volumetric reaction rate (colour contours) and the fluctuating axial velocity (gray scale). The hydrodynamic modulation of the flow inside the channels due to the diaphragms is clearly visible. High velocity pockets (white) generated at the diaphragm lips are convected towards the flames at the mean flow velocity. These pockets result from the velocity field induced by elongated annular vortices shed at the diaphragms lips and triggered by the global incident acoustic modulation. The axially staggered diaphragms induce a phase delay $\Delta\varphi = 2\pi f \Delta l/\mathcal{U}_{cv}$ between the perturbations propagating in the two channels. In the present configuration, $\mathcal{U}_{cv} \simeq (d_p/d_d)^2 \bar{u}_0 = 5.3\,\mathrm{m\,s^{-1}}$, $\Delta l = 3\,\mathrm{mm}$ and $f = 650\,\mathrm{Hz}$, yielding $\Delta\varphi \simeq 2.3$. This phase induces a flame motion which is not far from phase opposition ($2.3 \simeq 6\pi/8$). When one flame is expanding, the other is contracting. The maximum displacement of the flames is observed at phase angles $4\pi/7$ and $10\pi/7$. The present calculation does not correspond to the nominal frequency (the one leading to a perfect phase opposition), because the propagation velocity was not initially known. However, the applicability of the DPC concept is suitably demonstrated by this simulation.

3.2. Experimental results

The effect of the DPC is now examined experimentally in a multipoint injection configuration featuring strong self-sustained oscillations [17, 18]. The setup comprises 420 small conical flames which are anchored near the orifice lips of a perforated plate (Fig. 4a). An upstream manifold serves to feed this multipoint injector with a lean methane-air mixture. It was checked that

This is a pre-print version. Published in *Proceedings of the Combustion Institute*, Volume 32 (2009), p. 3163-3170, DOI: 10.1016/j.proci.2008.05.051

this manifold was acoustically isolated from the resonant cavity and that it provided uniformly premixed reactants. Equivalence ratio fluctuations, which can also drive combustion instabilities [25], are indeed not considered in this study, but one may infer that the DPC could favor mixing in such situations – in addition to the dynamic compensation – stabilization of the system. The DPC concept was implemented in the 420 channels of the perforated plate to provide a dynamic compensation of flow perturbations. Diaphragms were inserted in these perforations at different axial locations as explained in section 2. The geometrical characteristics of the DPC are nearly the same as those used in the simulation. The channel diameter $d_p = 2\,\text{mm}$ also corresponds to that used in [17, 18], the diaphragm diameter is $d_d = 1.2\,\text{mm}$, the stagger distance between type 1 and 2 channels is fixed to $\Delta l = 4\,\text{mm}$ with axial positions of the diaphragms in the channels $l_1 = 4$ and $l_2 = 8$ mm. An upstream modulation of the flow is generated by a loudspeaker fed with a signal delivered by a synthetizer. Flow conditions are the same as in the simulation : $\bar{u}_0 = 1.9\ \text{m}\,\text{s}^{-1}$ and $\phi = 0.86$.

Axial velocities in the fresh stream were measured at type 1 and 2 channel outlets by means of LDV (see [17] for more experimental details). Flow modulation frequencies were fixed at 500 and 650 Hz. With the present geometrical and flow conditions, the optimal dynamic compensation is expected at $f_n \simeq \bar{u}_0(d_p/d_d)^2/2\Delta l = 663.8$ Hz. It was found that the best compensation occurs at a frequency imposed by the loudspeaker equal to 650 Hz (Fig. 7). This figure also shows that the off design configuration corresponding to $f = 500$ Hz also yields out of phase velocity signals at the type 1 and 2 injectors outlets. Experimental results obtained under forced flow experiments and

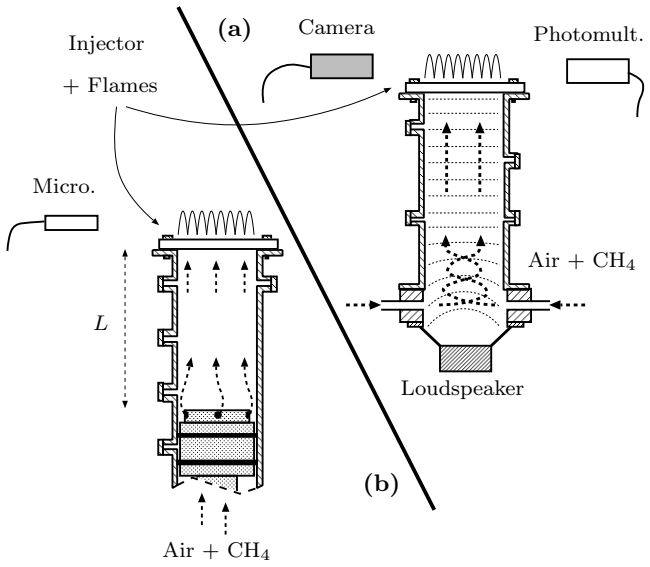

Figure 4: **(a)** Measurements of the flame response to upstream perturbations under external modulation. **(b)** Experimental characterization of acoustic radiation from the different perforated plates under autonomous operation.

This is a pre-print version. Published in *Proceedings of the Combustion Institute*, Volume 32 (2009), p. 3163-3170, DOI: 10.1016/j.proci.2008.05.051

presented next correspond to this slightly off-design configuration, where the frequency imposed by the loudspeaker is $f = 500$ Hz. This shows that the dynamic compensation is still effective.
The flame response to the upstream modulation of the flow is successively examined with the standard injector without diaphragms and then with an injector including the DPC. Equivalence ratio, mass flow rate, modulation amplitude and frequency are the same in both situations.
Flame fronts motion is recorded with a camera and light emission of hydroxyl radicals present in the flames is acquired by means of a photomultiplier equipped with a narrowband filter. In the present lean premixed configuration, this signal is proportional to the global heat release rate in the reaction zone which constitutes the driving source of thermo-acoustic instabilities.
Flame visualizations with and without dynamic compensation are given in Fig. 6. Each picture of the two sequences was obtained by zooming with the camera on two flames rows, but the experiments were carried out with a perforated plate featuring more than 10 rows of type 1 and type 2 channels. Thirteen instantaneous snapshots were recorded at successive phase angles of an oscillation cycle. It is clear that (1) When the standard injector is used, flames fronts move in a coherent fashion, and (2) When the dynamic compensation is provided by the phase converter system, flame motions are out of phase. When one of the flames is stretched the other retracts.
Effectiveness of dynamic compensation corresponding to the flames sequence presented in Fig. 6 is quantitatively demonstrated in Fig. 7 which shows time traces of the light emission signals recorded with the photomultiplier. These signals are proportional to the heat release rate of the entire set of flames. Open triangles correspond to the standard injector, while black circles stand

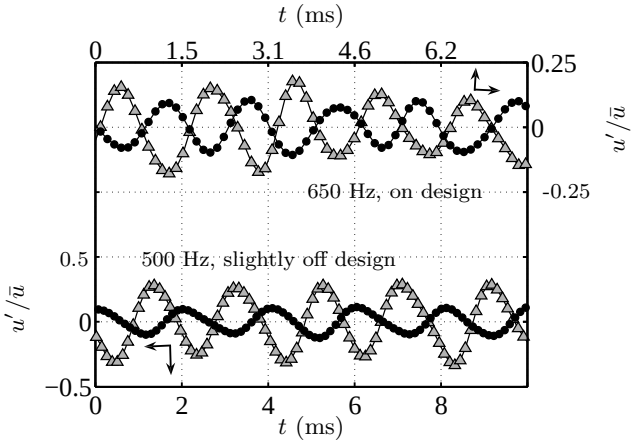

Figure 5: Time tracks of the normalized fluctuating axial velocity $u'/\bar{u}$ at the channel outlet recorded under forced flow experiments with flames and DPC injection. The velocity signals are acquired by means of a LDV setup. The measurement point is located 1 mm above the injection channel outlet, at the base of one of the flames. The top traces correspond to a modulation frequency of 650 Hz, while the bottom ones to a driving frequency of 500 Hz. In each couple of traces, the gray triangles and the black circles tracks respectively correspond to axial flow velocity at type 1 and type 2 injection channels outlet.

This is a pre-print version. Published in *Proceedings of the Combustion Institute*, Volume 32 (2009), p. 3163-3170, DOI: 10.1016/j.proci.2008.05.051

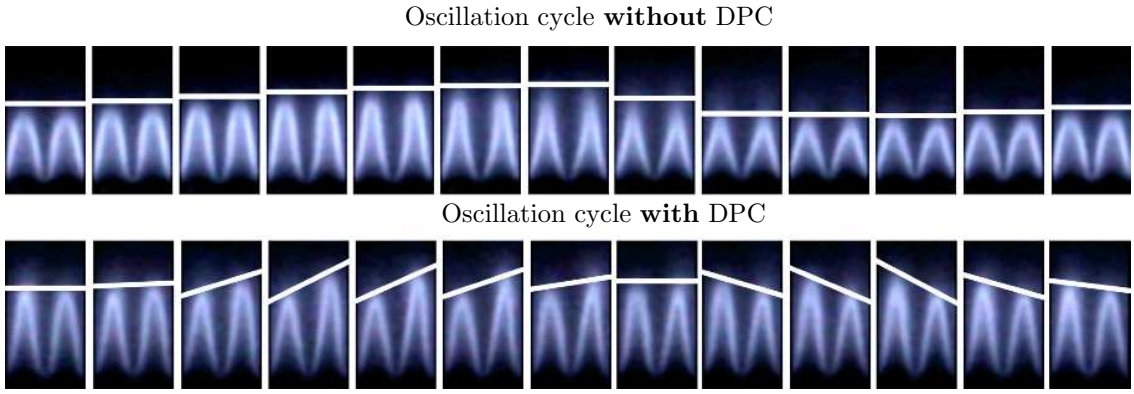

Figure 6: Flame visualisations under external modulation in the case of a multipoint injector without diaphragms (top) and with the diaphragms (bottom). The forcing frequency is 500 Hz and the modulation amplitude is 10 percent of the mean flow velocity. The figure shows images recorded at 13 successive phases during a cycle of oscillation. White lines designating the flames tips have been superimposed to the pictures in order to improve the flames motion perception.

for that equipped with the DPC. Without diaphragms, the heat release rate feature a sinusoidal shape indicating that the flames collectively respond to the acoustic excitation imposed by the loudspeaker. In contrast, when the DPC is used, the signal is nearly constant indicating that the global response of the flames is neutral. This experiment shows that the DPC completely suppresses the coherent response of the combustion region at the off-design frequency of 500 Hz

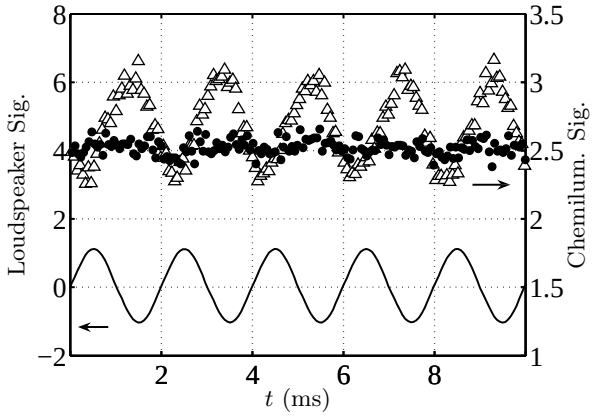

Figure 7: Time traces recorded under external modulation (f = 500 Hz) with (•) and without (△) the presence of diaphragms. The bottom trace corresponds to the driver unit excitation, the others are respectively the flame response with and without DPC system obtained by measuring the light intensity radiated by OH* radicals. This last signals are proportional to the heat release rate.

This is a pre-print version. Published in *Proceedings of the Combustion Institute*, Volume 32 (2009), p. 3163-3170, DOI: 10.1016/j.proci.2008.05.051

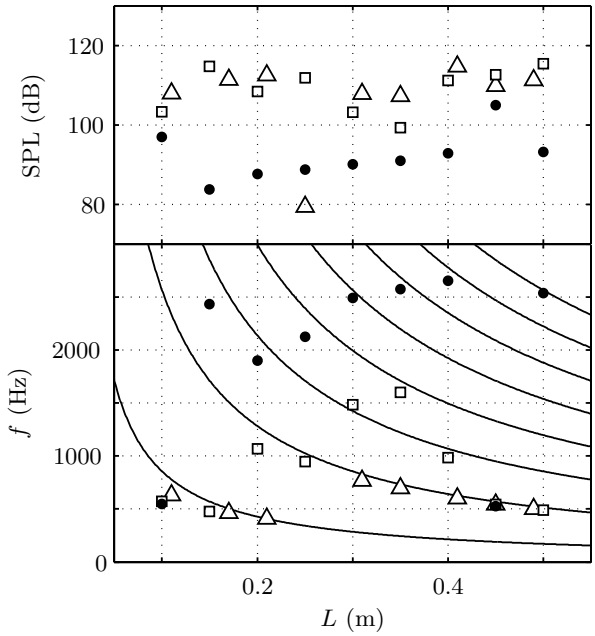

Figure 8: Top : Sound pressure level radiated by the system equipped with a standard perforated plate (△), equipped with a perforated plate including a phase convertor (•) and with diaphragms positioned at the same distance from the outlet (□). Bottom : Peak frequency radiated by the system plotted as a function of the upstream manifold size L. Mean flow velocity in each orifice 3.5 $\mathrm{m\,s^{-1}}$. Equivalence ratio : 0.86. The burner can be assimilated, in a first approximation, to a quarter wave resonator with theoretical eigenfrequencies $f_k = (2k+1)c/4L$ plotted as solid lines.

and operates as expected in a band around the nominal value $f_n = 663.8$ Hz.

4. Autonomous operation

It is then logical to consider the system in self-sustained regimes and see if the occurrence of oscillations is hindered.

The experimental configuration shown in Fig. 4b is now used (see also [18]). The dominant frequency of the noise radiated by the flames is plotted in Fig. 8 together with the sound pressure level, as a function of the manifold size, for different injection systems. The burner is successively equipped with (1) the reference plate without DPC system (△), (2) a perforated plate featuring diaphragms located at the same axial location 8 mm upstream from the channel outlet (□), and (3) the DPC with staggered diaphragms 4 and 8 mm upstream from the channels outlet (•). Systematic experiments are carried out at constant mass flow rates corresponding to a bulk velocity inside the channels $\bar{u}_0 = 3.5\ \mathrm{m\,s^{-1}}$ and a equivalence ratio $\phi = 0.86$. The upstream manifold size L is varied to sweep the different unstable modes of the system. Conditions used here yield a nominal dynamic compensation frequency $f_n \simeq \bar{u}_0(d_p/d_d)^2/2\Delta l = 1215$ Hz. The top graph in Fig. 8 indicates that

This is a pre-print version. Published in *Proceedings of the Combustion Institute*, Volume 32 (2009), p. 3163-3170, DOI: 10.1016/j.proci.2008.05.051

the DPC system (•) effectively reduces the amplitude of oscillation. Over a broad range of duct sizes the sound pressure level is reduced by 10 to 20 dB. The system essentially suppresses the low frequency oscillation but the geometry is nearly perfect and higher order modes arise. The bottom graph in Fig. 8 indicates that high frequency oscillations are observed around 2 kHz. Such high frequencies are undesirable in practical applications, and this reduces the value of the system. However, this effect will have less impact in practice because (1) the corresponding levels are much smaller than those corresponding to the lower frequency modes, (2) high frequency oscillations can be suppressed with additional damping devices such as perforated liners, (3) the device used in the present experiments is an idealized version of practical systems featuring more complex geometries which will filter out the higher frequencies. In most practical situations, problem arise in the low frequency range where oscillations are most difficult to eliminate and this is exactly what the phase convertor can do. One may finally wonder if damping is induced by actual dynamic compensation or simply by acoustic dissipation due to the vortex generation at the diaphragm lips where energy is converted from the acoustic to the hydrodynamic field. Experiments carried out with the diaphragms located at the same axial location (□) yield noise levels similar to those of the basic configuration (△), indicating that the dynamic compensation is actually operating.

5. Conclusion

A new strategy for passive control of combustion instabilities is proposed for systems featuring multiple flames. In contrast with classical acoustic absorber devices, the method relies on a modification of the flame dynamics. It is shown that by slightly modifying the feeding channels of a multipoint injector, it is possible to create a combustion region which is insensitive to acoustic perturbations and responds in a neutral fashion to incoming flow perturbations. This is achieved by a dynamic phase converter (DPC) which is materialized by placing staggered diaphragms in adjacent channels of a multipoint injector. Using this arrangement, large wavelength acoustic perturbations are converted into hydrodynamic disturbances of shorter wavelengths. It is then possible to obtain a suitable phase between the different channels. The phase difference can be significant even if the stagger distance is small. When the convective mode impinges on the flames, this yields out of phase heat release rate fluctuations and the global response of the system is neutral. Simulations and experiments demonstrate that this principle is effective. The concept is quite generic and may be extended to other practical configurations. While the demonstration is carried out for plane acoustic perturbations one may infer that the DPC could be used to suppress azimuthal thermoacoustic couplings like those found in gas turbine applications. Practical implementations are the subject of a patent pending (no. 0705344). It is finally interesting to list advantages of this control solution : (1) Simple sizing method, (2) Low requirement in terms of space and mass, (3) Minor modification of the injection geometry, (4) Broad band effictiveness, (5) Minor modification of the steady state performance.

This is a pre-print version. Published in *Proceedings of the Combustion Institute*, Volume 32 (2009), p. 3163-3170, DOI: 10.1016/j.proci.2008.05.051

References

[1] K. R. McManus, T. Poinsot, S. Candel, *Prog. Energy Combust. Sci.* 19 (1993) 1–29.
[2] A. S. Morgans, S. R. Stow, *Combust. & Flame* 150 (2007) 380–399.
[3] K. C. Schadow, E. Gutmark, *Prog. Energy Combust. Sci.* 18 (1992) 117–131.
[4] G. A. Richards, D. L. Straub, E. H. Robey, *J. Prop. Power* 19 (5) (2003) 795–810.
[5] I. J. Hughes, A. P. Dowling, *J. Fluid. Mech.* 218 (1990) 299–335.
[6] N. Tran, S. Ducruix, T. Schuller, in: *AIAA paper, 13^{th} AIAA/CEAS Aeroacoustics Conference, 28^{th} AIAA Aeroacoustics Conference*, Rome, Italy, 2007.
[7] W. Krebs, S. Bethke, J. Lepers, P. Flohr, B. Prade, C. Johnson, S. Sattinger, in: *Combustion instabilities in gas turbines*, edited by Lieuwen, T. C. and Yang, V., American Institute of aeronautics and astronautics, Inc., 2005.
[8] J. M. DeBedout, M. A. Franchek, R. J. Bernhard, L. Mongeau, *J. Sound & Vib.* 202 (1997) 109–123.
[9] C. H. Wang, A. P. Dowling, in: *Advances in Combustion and Noise Control*, Cranfield University Press, 2005, pp. 45–64.
[10] T. Poinsot, A. Trouve, D. Veynante, S. Candel, E. Esposito, *J. Fluid Mech.* 177 (1987) 265–292.
[11] H. Hu, T. Saga, T. Kobayashi, N. Taniguchi, in: *6^{th} Triennal Symposium on Fluid Control Proceedings*, Sherbrooke, Canada, 2000.
[12] C. O. Paschereit, E. Gutmark, in: *AIAA paper 2002-1007, 40^{th} AIAA Aerospace Sciences Meeting and Exhibits*, Reno, US, 2002.
[13] E. J. Gutmark, F. F. Grinstein, in: *AIAA paper, 35^{th} AIAA Aerospace Sciences Meeting and Exhibits*, Reno, US, 1997.
[14] U. Hedge, D. Reuter, B. Zinn, in: *AIAA paper 89-0979, AIAA 2^{nd} Shear Flow Conference*, Tempe, AZ, USA, 1989.
[15] R. C. Steele, L. K. Cowell, S. M. Cannon, C. E. Smith, *Journal of Engineering for Gas Turbines and Power, ASME Trans.* 122 (2000) 412–419.
[16] T. Scarinci, in: *Combustion instabilities in gas turbines*, edited by Lieuwen, T. C. and Yang, V., American Institute of aeronautics and astronautics, Inc., 2005.
[17] N. Noiray, D. Durox, T. Schuller, S. Candel, *Combust. & Flame* 145 (3) (2006) 435–446.
[18] N. Noiray, D. Durox, T. Schuller, S. Candel, *Proc. Combust. Inst.* 31 (1) (2007) 1283–1290.
[19] L. Selle, G. Lartigue, T. Poinsot, R. Koch, K. Schildmacher, W. Krebs, B. Prade, P. Kaufman, D. Veynante, *Combust. & Flame* 137 (4) (2004) 489–505.
[20] T. Schönfeld, M. Rudgyard, *AIAA J.* 37 (11) (1999) 1378–1385.
[21] C. M. Vagelopoulos, F. N. Egolfopoulos, C. K. Law, *Proc. Combust. Inst.* 25 (1994) 1341–1347.
[22] T. Poinsot, D. Veynante, *Theoretical and Numerical Combustion*, Edwards, Philadelphia, 2001.
[23] O. Colin, M. Rudgyard, *Journal of Computational Physics* 162 (2) (2000) 338–371.
[24] A. L. Birbaud, D. Durox, S. Ducruix, S. Candel, *Phys. Fluids* 19 (1) (2007) 013602.
[25] T. Sattelmayer, *Journal of Engineering for Gas Turbines and Power, ASME Trans.* 125 (2003) 11–19.

This is a pre-print version. Published in *Proceedings of the Combustion Institute*, Volume 32 (2009), p. 3163-3170, DOI: 10.1016/j.proci.2008.05.051